Materials Today Communications 39 (2024) 108656

Contents lists available at ScienceDirect

Materials Today Communications

journal homepage: www.elsevier.com/locate/mtcomm

On the vibrational behavior of the conventional and hetero-junction carbon nanotubes

Ali Ghavamian [a,*], Sourish Banerjee [a], Moones Rahmandoust [b], Andreas Öchsner [c]

[a] School of Engineering, University of Southern Queensland, Toowoomba 4350, Australia
[b] Protein Research Center, Shahid Beheshti University, Velenjak, Tehran 1983969411, Iran
[c] Faculty of Mechanical and Systems Engineering, Esslingen University of Applied Sciences, Esslingen 73728, Germany

ARTICLE INFO

Keywords:
Carbon nanotube
Hetero-junction structure
Natural Frequency
Vibration
Finite element method

ABSTRACT

The shortcomings and insufficiency in the state-of-the-art investigations about the resonance in the hetero-junction carbon nanotubes with respect to the number of models and connection types highlight the necessity of a comprehensive study of the resonance frequency of these nanostructures for applications of these nanomaterials in nanodevices, such as nano-scale electromechanical systems (NEMS) and NEMS-based resonators. Hence in this study, 50 conventional and 73 hetero-junction middle-length (15 nm) carbon nanotubes, with armchair-armchair, zigzag-zigzag, armchair-zigzag, armchair-chiral, zigzag-chiral and chiral-chiral connections, were modeled. Then, the resonance in their structure was comprehensively studied using the finite element method to present a more reliable estimated range for the natural frequency (fundamental frequency) of hetero-junction carbon nanotubes. The analysis showed that the natural frequency of conventional carbon nanotubes lies in the range of 7.09 and 48.75 GHz. An inverse correlation between this quantity and the aspect ratios of the conventional carbon nanotubes was found, leading to proposing a mathematical relation for the prediction of such an inverse correlation. The natural frequency of hetero-junction carbon nanotubes oscillated between 4.04 and 60.20 GHz. The results revealed that the natural frequency of hetero-junction carbon nanotubes lies outside the frequency range of their constructive carbon nanotubes and majorly depends on the boundary conditions and the difference between the diameters of the connected tubes. Finally, it was observed that the existence of an armchair carbon nanotube in the structure of hetero-junction models improves their vibrational stabilities.

1. Introduction

The worldwide desire for time, cost, and energy saving in the modern world has glorified the necessity of developing new tools with enhanced functionalities and efficiencies. Among all aspects of the new tools design, the material selection has been a critical step in designing man-made objects with enhanced functionalities and efficiencies. In this sense, nanomaterials have shined as promising materials with novel, unique, and application-ready properties in the industry. Since the discovery of carbon nanotubes (CNTs) in 1991 by Iijima [1], universal attention has been drawn to these carbon-based nanomaterials, owing to their advantageous and highly tunable properties as well as their application potentials in various nanoindustry fields.

Useful mechanical characteristics such as lightness as well as high stiffness, strength, and aspect ratio have introduced the CNTs as attractive reinforcements in the structure of composite materials [2]. Moreover, these nanostructures are also used as high-sensitivity microbalances [3], gas and molecule sensors [4], field emission type displays [5], tiny tweezers for nanoscale manipulation [6], probes in scanning probe microscopy and atomic force microscopy instrumentation [7] with the additional advantage of a chemically functionalized tip, as well as their application in hydrogen storage devices, due to their high surface-volume ratio [8]. Finally, due to the relatively low toxicity and nonimmunogenic behavior of CNTs, these nanomaterials were also

Abbreviations: CNTs, Carbon Nanotubes; SWCNTs, Single-Walled Carbon Nanotubes; HJCNTs, Hetero-junction carbon nanotubes; FEM, Finite Element Method; NEMS, nano-scale electromechanical systems; CVD, Catalytic Vapor Deposition; AA, Armchair-Armchair; ZZ, Zigzag-Zigzag; AZ, Armchair-Zigzag; AC, Armchair-Chiral; ZC, Zigzag-Chiral; CC, Chiral-Chiral.

* Corresponding author.
E-mail addresses: ali.ghavamian@unisq.edu.au (A. Ghavamian), Sourish.banerjee@unisq.edu.au (S. Banerjee), rahmandoust.moones@gmail.com (M. Rahmandoust), andreas.oechsner@hs-esslingen.de (A. Öchsner).

https://doi.org/10.1016/j.mtcomm.2024.108656
Received 25 November 2023; Received in revised form 12 March 2024; Accepted 15 March 2024
Available online 21 March 2024

introduced to the world of nanomedicine [9] and for possible environmentally friendly applications.

Synthesis, purification, and functionalization process are the three basic steps in the industrial fabrication of CNTs. Historically, different approaches, i.e., arc discharge, laser ablation, catalytic chemical vapor deposition (CVD) processes, flame synthesis, and silane solution methods have been used for synthesizing the CNTs [10] among a dozen others.

Among all nanodevices, nano-scale electromechanical systems (NEMs) can also present natural frequencies in the microwave range as high as 100 GHz [11]. The distinguishing properties of these devices have highlighted their applications as force sensors, chemical sensors, biological sensors, and ultrahigh frequency resonators to play an important role in the future of computing and sensing fields. Owing to the application of NEMS-based devices as resonators, they are operated at a high frequency up to 1 GHz, when their sizes reach about 100 nm, providing extreme sensitivity. Therefore, materials with high frequencies are required to provide high sensitivity for these devices [12].

Si and GaAs are the two extensively materials used in the fabrication of NEMS, due to a high Young's modulus of around 100 GPa [13]. However, they are losing their popularities as they cannot fully satisfy the NEMS requirements due to the dominance of surface effects, such as surface oxidation and reconstruction, and thermoelastic damping causing to fail to achieve the anticipated high-quality factors. The performance of silicon-based NEMS actuators was also influenced by their limitations in strength and flexibility [12].

Instead, the outstanding and tunable properties of CNTs as well as their particular characteristics, i.e., nearly one-dimensional structures with high aspect ratios, nearly perfect-terminated surfaces and high ratios of Young's modulus to density which provide the CNTs with high resonance frequency can relatively compensate for the shortcoming of Si and GaAs, and introduce these nanomaterials ideal for application in NEMS [12] which could also benefit from low toxicity of the CNTs [9] for environmental applications. The significant advances in growth, manipulation and knowledge of the properties of CNTs have also introduced them as the most promising building blocks for the next generation of NEMS [12] and have encouraged many scholars to investigate their vibrational behavior under the cantilever or clamped-clamped boundary conditions as in most cases, the interesting properties of the NEMS devices typically emanate from the behavior of the active parts when they are in the forms of cantilever or clamped-clamped beams with dimensions at the nanometer scale [13].

1.1. Literature review: vibrational properties of conventional and defective CNTs

With regards to the high vibrational stability of the CNTs, these nanostructures have been employed in nanodevices for their reinforcement while enhancing their vibrational behavior. For instance, Al-Furjan et. al. [14] reported a reduction of 50% and 33% in dynamic deflection and flexural moment as a result of CNT reinforcement in the wave-piercing catamaran beam elements, respectively. The nonlinear static and free vibration analysis of the Euler-Bernoulli composite beam by Mohammadimehr and Alimirzaei [15] showed an increase in the dimensionless nonlinear natural frequency and stiffness of the beam as a result of the reinforcement by functionally graded single-walled carbon nanotubes (SWCNTs). Mellouli et al. [16] also confirmed the influence of the CNT volume fraction on enhancing the vibrational behavior of functionally graded CNT-reinforced shell structures. An analytical study by Dinh Dat et al. [17] emphasized an increase in the natural frequency and a decrease in the frequency ratio of a smart sandwich plate as a result of CNT addition. Ghorbanpour Arani et al. [18] also reported an increase in the vibrational stability of a CNT-reinforced sandwich plate due to the enhancement of the stiffness of the system by CNT reinforcement. They reported an increase of about 29.36% in dynamic deflection of the rhombic plate as a result of waviness and random distribution of CNTs. However, they pointed out that the random distribution appeared to be more important than the waviness parameter for CNTs with respect to mechanical response. It was also concluded that by increasing the aspect ratio, the CNT's volume percent shows a greater impact on the dimensionless frequency.

Adding a proper volume fraction of CNTs into the structure of carbon-reinforced composites not only enhances their stiffness and strength but also improves their vibrational behavior as the most effective passive of active vibration absorbers by converting them to energy [19]. Wan et al., [20] investigated the effects of reinforcing a hybrid nanocomposite viscoelastic rhombic plate with CNTs and carbon fibers on the post-buckling behavior, free and forced vibration as well as energy absorption characteristics. Wang et al. [21] reported that an increase in the volume fraction of CNTs improves the natural frequency of nanocomposites. Fazilati et al. [22] mentioned a slight increase in the natural frequency of the nanocomposite as a result of the CNTs agglomeration occurrence. Babaei [23] emphasized the importance of the CNT distribution pattern and stiffness of the elastic foundation on the natural frequency of the nanocomposite. Nopour et al. [24] introduced CNTs as one of the most extensively used candidates for enhancing high-cycle fatigue behavior and vibrational characteristics of nanocomposites for energy absorption purposes.

Due to the costs and technology limitations in experimental approaches, theoretical (analytical and computational) methods have been widely employed for vibrational characterization of the CNTs as standalone materials. Among the theoretical techniques, molecular dynamics and analytical mechanics have been considerably applied. However, long computational time, modeling size limitation and low accuracy for many molecular dynamics simulations, and the limitations in the definition of some model parameters in the analytical approaches have persuaded many scholars to employ the computational techniques, e.g., finite element method (FEM) which has recently earned worldwide popularity to overcome such issues [25]. Table 1 provides a brief overview of different approaches from literature by different scholars for the investigation of the vibrational properties of conventional CNTs.

Aside from the ranges predicted for the natural frequency of the defect-free CNTs, it has been reported that the defects in the structure of the CNTs result in a lower natural frequency. Ghavamian and Öchsner [37] confirmed a decrease in the resonance stability of the CNTs, under the influence of different atomic defects, i.e., vacant sites, Si-doping and perturbation, and proposed mathematical relations for prediction of the influence of such defects. Such a decreasing effect of carbon vacancies and the effect of their locations were also confirmed by Ebrahim Zadeh et al. [40]. Selim and El-Safty [41] reported that the initial curvature in the CNT structures causes a decrease in their natural frequencies. The research by Parvaneh et al. [42] expressed that the vacant sites and Stone-Wales defect in the structure of sufficiently long single-walled carbon nanotubes do not have a considerable effect on their natural frequencies at the Euler mode. However, for short-length nanotubes with an aspect ratio of approximately 4.5 and up, this influence is much greater. At shell mode, a critical influence of defects on the natural frequency of the CNTs was witnessed and thus, the application of defect-free CNTs with small aspect ratios was suggested. Due to the high-frequency requirements in the CNTs for usage in NEMS, an exact prediction of their natural frequencies was also emphasized concerning the occurrence of the shell modes. Beside the location effects of the defects, local changes in the material structure by Stone-Wales defects caused a greater impact on the natural frequency of the CNTs at shell mode when compared with carbon vacancies.

A glance at the results from many other scholars clearly shows that the natural frequency of CNTs is a length-sensitive quantity and has an inverse correlation with the length of the tubes. Chwal [43], confirmed such an inverse correlation and reported the eigenfrequency of the CNTs with 2.83–28.3 nm lengths between about 1800 and less than 100 GHz for (5,5) and for (10,10) CNTs, between more than 2000 and less than

Table 1
Literature on the vibrational properties of CNTs.

CNT type	Methodology and approaches	Obtained results (natural frequency (f))	Researcher
Defect free conventional	Atomic force microscope (AFM)	Natural frequency of a clamped–clamped CNT was measured up to 3 GHz.	San Paulo et al. [26]
Defect free conventional	Non-local theories	Size-effects on the vibration analysis of SWCNTs was studied and the natural frequency SWCNTs was obtained as: $127.2 < f < 804.2$ GHz for Armchair SWCNTs $9.2 < f < 1183.6$ GHz for Zigzag SWCNTs	Ansari and Sahmani [27]
Defect free conventional	Continuum mechanics	Natural frequency of SWCNTs was reported as: $7 < f < 300$ GHz under clamped-free boundary conditions $40 < f < 1700$ GHz under clamped-clamped boundary conditions $20 < f < 800$ GHz under simply-supported boundary conditions $20 < f < 800$ GHz under free-free boundary conditions	Lee et al. [28]
Defect free conventional	Molecular structural mechanics	Natural frequency of SWCNTs was obtained as: $13.1 < f < 37.6$ GHz for armchair $9.38 < f < 48$ GHz for zigzag	Lü et al. [29]
Defect free conventional	Molecular mechanics (MM)	Natural frequency of short-length CNTs under clamp-free and clamp-clamp boundary conditions was studies and reported as: 10 GHz $< f < 1.5$ THz	Li and Chou [30]
Defect free conventional	Molecular mechanics (MM)	Natural frequency of SWCNTs was obtained as: $70 < f < 2400$ GHz for different aspect ratios	Chowdhury et al. [31]
Defect free conventional	Molecular dynamics (MD)	Natural frequency of SWCNTs was obtained as: $220 < f < 1450$ GHz under different boundary conditions with the same length.	Hu et al. [32]
Defect free conventional	Finite element method	Natural frequency of zigzag double-walled was reported as: $25 < f < 250$ GHz	Fan et al. [33]
Defect free conventional	Finite element method	Natural frequency of SWCNTs of different length and diameters were obtained as: $12 < f < 718$ GHz for armchair CNTs $2 < f < 289$ GHz for zigzag CNTs	Sakhaee-pour et al. [34]
Defect free conventional	Finite element method	Natural frequency of SWCNTs was acquired as: $0.0145 < f < 0.0764$ GHz for armchair CNTs $0.0122 < f < 0.0448$ GHz for zigzag CNTs	Mir et al. [35]
Defect free conventional	Finite element method	Natural frequency of armchair and zigzag nanotubes had values about 23 GHz under cantilever boundary conditions.	Rahmandoust and Öchsner [36]
Defect free and defective	Finite element method	Mathematical relations were proposed for the prediction of natural frequency of single- and multi-walled CNTs as well as the following ranges were predicted: $23 < f < 51$ GHz for armchair CNTs $18 < f < 50$ GHz for zigzag CNTs	Ghavamian and Öchsner [37]
Defect free conventional	Finite element method	Natural frequency of armchair and zigzag SWCNTs of 5 nm long under clamped–free and clamped–clamped boundary conditions was obtained in the following ranges: $0.1 < f < 2.15$ THz for armchair CNTs $0.07 < f < 2.69$ THz for zigzag CNTs	Arghavan and Singh [38]
Defect free conventional	Finite element method	Natural frequency of SWCNTs was reported as: $2 < f < 712$ GHz for armchair CNTs $1.5 < f < 981$ GHz for zigzag CNTs	Fakhrabadi et al. [39]

100 GHz, respectively. The results by Miyashiro et al. [44] demonstrated a range of about 40000 and 60 GHz for the natural frequency of 2.5–30 nm long SWCNTs, respectively. Fatahi-Vajari and Azimzadeh [45] also presented the range of 2.1 and 0.1 THz for the forward frequency of SWCNTs with the lengths varying between 5 and 30 nm.

1.2. Literature review: applications and vibrational properties of hetero-junction CNTs

The experimental observations have shown that it is possible that two CNTs connect together through a heptagon-pentagon knee and construct a hetero-junction carbon nanotube (HJCNT). These nanostructures can experimentally be constructed by predetermined temperature-mediated growth during CVD [46]. Also, HJCNTs can be produced by connecting two neighboring CNTs to each other vie a high electric field [47] or the Joule heating process [48].

Behaving like nanoscale metal/semiconductor or semiconductor/semiconductor junctions, it was proposed that the hetero-junction CNTs could be employed as the entirely carbon-made building blocks of nanoscale electronic devices, e.g., rectifying diodes and switches [49]. Other applications of hetero-junction CNTs, i.e., as nano-pores and nano-sieves in transport problems [50], blood vessels or flow sensors in the nano-measurement methods [51] and efficient solar cells [52,53] while benefitting from some particular outstanding properties of the CNTs, e.g., high mobility, excellent air stability, flexibility, ultra-high light absorption ability, high electrical conductivity and other interesting CNT mechanical properties, i.e., lightness, high stiffness and large aspect ratio [54] have been reported by many scholars.

In recent years, the application of carbon based nanostructures in the field of high performance nanomechanical sensors has drawn special attentions. For instance, the pillared graphene [55] and diamond nanothreads [56] structures which offer high mass sensitivity up to 10^{-24} g have been proposed as appealing candidates for designing mass nanosensors.

With regards to the fact that the vibration-based mechanical sensors operate based on measuring the frequency shift caused by the interactions with the external environment, the vibrational properties of the CNTs have highly been regarded as the CNT-based resonators are very sensitive to the external mass and even a small mass which can change the frequencies of such resonators [57]. In this sense, the vibrational characteristics of hetero-junction CNTs which inherit the mechanical properties of their constructive nanotubes has recently been studied either as stand-alone materials or building blocks in the structure of NEMS, e.g., a mass sensor.

Scarpa et al. [58] evaluated the vibrational behavior of hetero-junction oscillators by a hybrid atomistic-continuum approach. Based on their results, unusual selective mass sensing capabilities depending on the geometry and the type of boundary conditions of the specific nanostructure were observed which suggests a possible application of these nanomaterials as novel types of nanosensors, offering

different types of information and sensing capabilities based on the position of the mass or applied forces, and filtering characteristics of the dynamic response, in terms of the type of applied boundary condition.

In another research, a hybrid FEM-atomistic-continuum approach was used by Scarpa et al. [59] to investigate the dynamic properties of HJCNT oscillators. They found out that the natural frequency and mode shapes of HJCNTs are influenced by the relative length of the connecting CNTs versus the junction length. The significantly different frequency shift, shown by hetero-junctions under different boundary conditions (clamped-clamped, clamped-free) demonstrated a promising potential for these nanostructures to be employed in NEMS. The natural frequency of an HJCNT of 10 nm length was also obtained about 20 GHz and it was concluded that an increase in the length of the HJCNT leads to a decrease in their natural frequency.

Mohammadian and his colleagues [60] performed a two-phase investigation on the vibrational properties of HJCNTs with and without attached mass (as a cantilever mass sensor). Their results demonstrated that the frequency shift of an HJCNT increases by increasing the attached mass or decreasing the length. The cantilever HJCNT also appeared more efficient in sensing light or heavy masses than uniform CNTs due to having higher relative frequency shifts. The fundamental frequency of a cantilever HJCNT-mass system showed much less dependency on the magnitude of the attached mass when compared with the second and higher frequencies. They eventually introduced HJCNTs as new and more efficient mass nanosensors, compared with uniform CNTs.

Apart from the studies on the vibrational behavior of HJCNTs as parts of nanodevices, several theoretical investigations have been performed for vibrational analysis of these nanomaterials as stand-alone materials. A nonlocal theory was employed by Filiz and Aydogdu [61] to investigate the axial vibration of hetero-junction CNTs by nonlocal constitutive relations of Eringen to study the effects of chirality, length and diameter of corresponding CNTs on the vibrational properties of hetero-junctions. According to their results, the axial vibration frequencies of CNT hetero-junctions were found to be highly overestimated by the classical rod model due to ignoring the effect of small length scale. They finally concluded that the frequency parameter of hetero-junction CNTs can be optimized by changing length and cross section of each segment.

Mohammadian et al. [62] performed several investigations on the vibrational behavior of hetero-junction CNTs. In his first research, he employed a molecular mechanics technique, combined with the FEM to model straight and non-straight HJCNTs and investigate their first four natural frequencies and their mode shapes, and the effects of connecting region length on the frequencies of these nanostructures under different boundary conditions. For clamped-free boundary conditions, the first and second natural frequencies of HJCNTs, with a length of 14 nm, were obtained in the range of 39 and 47 GHz while such a quantity was acquired between 120 and 245 GHz for clamped-clamped boundary conditions, respectively. The natural frequency of HJCNTs was also found to have an inverse correlation with their length.

Later on, Mohammadian et al. [63] evaluated the vibrational characteristics of the HJCNTs under the influence of the atomic defects by FEM. The natural frequency of HJCNTs was found to oscillate between 20 and 170 GHz. The maximum values for the first four frequencies were found when the connecting region location is located near the thinner end while for the fifth frequency, the peak value occurred when the connection was almost in the middle of HJCNT. Their results also elucidated that all of the three defects (carbon vacancy, Si-doping, and perturbation) decrease the fundamental frequency of the structure. However, the frequency shift of HJCNTs showed more sensitivity to the vacancy defect, compared with the other two defects.

In another research, Mohammadian et al. [64] evaluated the lateral vibration of an embedded HJCNT via introducing a new single-stepped nonlocal strain gradient Rayleigh beam model. The frequency of these nanomaterials also appeared to be influenced by the type of adopted higher-order boundary conditions and always remained constant when the two scale parameters were identical. In addition, the nonlocal parameter for a specific value of the Pasternak foundation parameters did not show any effect on the frequency of clamped-free and clamped-clamped HJCNTs.

Motamedi et al. [65] studied the natural frequency of zigzag-zigzag (ZZ) HJCNTs by the molecular mechanics approach. Their results revealed that clamping the larger end of an HJCNT leads to an increase in natural frequency while clamping the smaller end of HJCNTs decreases the natural frequency. The resonance frequency of cantilever hetero-junction CNT with a length of 20 nm was reported to be 600 GHz and 200 when thinner and thicker ends were fixed, respectively.

Roy et al. [66] investigated the vibrational behavior of various boron nitride nanotubes, CNT-based hetero-junctions, and van der Waals hetero-structures. According to their results, compared to the pristine SWCNT, an increase in the number of boron nitride rings was observed to cause the 13.6% and 6.67% reduction in the resonant frequency of the hetero-junctions for the clamped-clamped and clamped-free boundary conditions, respectively. Similar to the pristine SWCNT, the hetero-junctions demonstrated an increase in resonant frequency with an increase in the inherent strain percentage. Likewise, the increase in inherent strain percentage showed an influence on the resonant frequency of the different van der Waals structures. A strong inverse correlation between the temperature and the resonant frequency in the hetero-junctions and the van der Waals hetero-structures was also witnessed.

Imani Yengejeh et al. [67] studied the vibrational behavior of nine straight HJCNTs by the FEM method under cantilever boundary conditions and reported the natural frequency of armchair-armchair (AA) HJCNTs in the range of 15 and 140 GHz and the one for ZZ HJCNTs in the range of 17–180 GHz. They also pointed out that the fundamental frequency of straight HJCNTs lies within the range of their constituent CNTs. Moreover, the eigenvalues of straight HJCNTs appeared to increase with increasing the chirality of CNTs.

Despite the considerable number of investigations on the properties of HJCNTs, their vibrational properties have been less addressed. In most of these investigations, the focus has only been on some hetero-junction connection types (straight connections), while the other possible connections (bent connections) have almost been neglected. Furthermore, only a few models of HJCNTs have been studied in previous investigations whose number does not seem to be sufficient to comprehensively understand their vibration behavior.

With regards to the fact that different structures of HJCNTs are constructed of various fundamental CNT configurations, connection types, kinks, and bending angles, and these factors as well as the boundary conditions setup have a determinant influence on the vibrational properties and response of these nanomaterials, a comprehensive study on the considerable number of HJCNTs with all possible connection types is required.

In this research, 73 straight and bent middle-length HJCNTs (15 nm), constructed of all possible connection types, i.e., including not only the AA, and ZZ types, which were addressed before [65,68], but also the armchair-zigzag (AZ), armchair-chiral (AC), zigzag-chiral (ZC) and chiral-chiral (CC) connections, accompanied by their fundamental constructive SWCNTs (50 models) of armchair, zigzag and chiral configurations with different diameters have been modeled. Then, their natural frequencies (fundamental or first natural frequencies) have been investigated under the cantilever boundary conditions. Such a study uniquely offers a more reliable range for the natural frequency of conventional and HJCNTs for the comparison and evaluation of the influential factors on the resonance behavior of these nanostructures for their promising applications in designing HJCNT-based mass nanosensors.

Owing to cost and technological limitations in performing experimental analysis of the HJCNTs' vibrations and the fact that the current research is limited to middle-length models (about 15 nm) under only cantilever boundary conditions with the negligence of small-scale

effects, the necessity of incorporation of small-scale effects as well as performing similar FEM-based study of the resonance behavior of short and long HJCNTs under other boundary conditions, e.g., clamped-clamped boundary conditions is highlighted and left to the future investigations to establish a comprehensive database of the resonance frequency of these nanomaterials for their proper applications in nanodevices.

1.3. Macro and atomic structure of homogenous and hetero-junction CNTs

The similarity between the atomic structure of CNTs and graphene enlightens the idea that an SWCNT can logically be imagined to be formed by rolling a graphene sheet into a carbon-built hollow cylinder or a CNT with a wall thickness which is generally assumed to be equal to the diameter of a single carbon atom (0.34 nm), with the outer diameter within the range of 1–50 nm and the overall length, often exceeding 10 μm [68]. Exemplary schematic features of a graphene sheet, unit cell, and SWCNT, illustrated in Figs. 1a to 1c, shows that similar to graphene sheets, carbon nanotubes are atomically structured of honeycomb-like hexagonal unit cells. Each unit cell is also constructed of six carbon atoms, each of which bonded to three neighboring carbon atoms by covalent C-C bonds with a bond length of 0.142 nm [68].

As illustrated in Fig. 1a, the configuration or type of a CNT is normally distinguished by its chirality, or helicity which is expressed by its corresponding chiral vector $\vec{C}_h$, expressed by Eq. (1), in terms of two

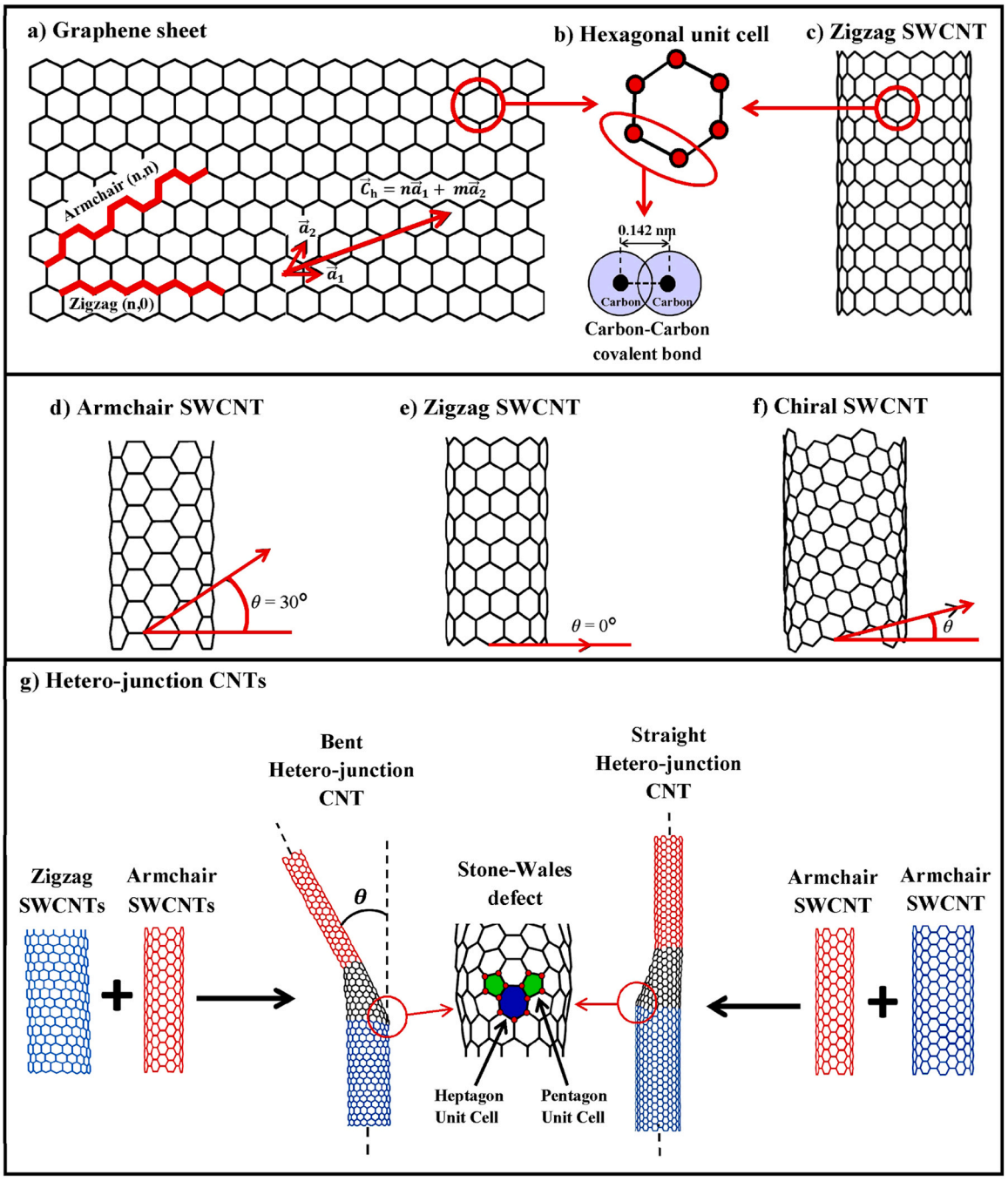

Fig. 1. (a), (b) and (c) schematics of grapheme sheet, hexagonal unit cell and zigzag SWCNT, respectively; (d), (e) and (f) armchair, zigzag and chiral SWCNTs, respectively; (g) Hetero-junction CNT structure and Stone-Wales defect. (*Source:* Obtained from [69]).

unit vectors $\vec{a}_1$ and $\vec{a}_2$ and two integers m and n (steps along the unit vectors), or the chiral or twisting angle θ by which the graphene sheet is assumed to be rolled into an SWCNT [70].

$$\vec{C}_h = n\vec{a}_1 + m\vec{a}_2 \quad (1)$$

There are three fundamental CNT configurations, i.e., armchair, zigzag, and chiral, based on the CNT's chiral vector or chiral angle, as shown in Figs. 1d to 1 f. In terms of the chiral vectors (m and n) or in terms of the chiral angle θ, an armchair CNT is created when $m = n$ or $\theta = 30°$. On the other hand, a zigzag CNT is formed when $\theta = 0°$ or $m = 0$ and finally, a chiral structure is constructed if $0° < \theta < 30°$ or $m \neq n \neq 0$. The radius of an SWCNT is also calculated by Eq. (2) where $a_0 = \sqrt{3}\ b$ and $b = 0.142$ nm which is the C-C bond length [70],

$$R_{CNT} = a_0\sqrt{m^2 + mn + n^2}\Big/2\pi \quad (2)$$

According to experimental observations, HJCNTs are constructed when two different CNTs connect to each other by a kink or bending knee. As demonstrated in Fig. 1g, the structures of the HJCNTs are almost similar to conventional CNTs as they are made of hexagonal carbon unit cells, except at the connection locations, where pentagon-heptagon cell pairs are formed (also known as Stone-Wales defects) to make the connection between the different CNTs possible [71,72].

Previous research in the literature demonstrates the fact that the mechanical properties of CNTs are widely influenced by any type of defects and the homogeneity removing factors, e.g., existence of the kink as well as its size and the bending angle in the structure of HJCNTs which generally depend on three factors, i.e., the connection shape, bending angle and the configuration of the corresponding constructive conventional CNTs of these nanostructures [69].

Based on the connection shapes, there are two types of straight and bent HJCNTs as illustrated in Fig. 1g. Straight HJCNTs are formed when the orientations of the two connecting CNTs are parallel and they are of the same configurations (two armchair or two zigzag CNTs), whereas a bent HJCNT is constructed when the two connecting CNTs have different orientations (e.g., AZ, AC and ZC) [73]. The bending can also be observed when two chiral CNTs with different chiralities connect to form CC HJCNTs.

Regarding the bending angles, there are two major types of large-angle bent HJCNTs (with a bending angle of about 36°) [74] and small-angle bent HJCNTs (with a bending angle of about 12°) [49,71]. With regards to the fundamental CNTs' configurations, six possible connection types, i.e., AA, ZZ, AZ, AC, ZC and CC connections between each two CNTs can construct the HJCNTs. Obviously, among the HJCNTs with these six connection types, those models with AA and ZZ connections are straight and the models with the other connections are bent. The CC HJCNTs, whose fundamental CNTs' chiralities are very close to each other and close to one of the main orientations of armchair or zigzag, appear to have very small bending angles in their structure and thus, they could approximately be treated as straight models [75].

2. Methodology

2.1. Finite element modelling of conventional and hetero-junction CNTs

In FEM simulation of CNTs, their structures are often considered to be constructed of honeycomb-like hexagonal unit cells which are made of C-C covalent bonds, connecting every six neighboring carbon atoms. For such a modeling, CNTs are assumed to be space-frame structures where the nodes represent carbon atoms and the action of the C-C bonds (length: 0.142 nm) is approximated by one-dimensional beam elements with six degrees of freedom at each node, i.e., three global displacements and three global rotations in the spatial network, following the Euler-Bernoulli beam theory which seems to be a more suitable choice, when compared to other element types, e.g., rod, spring and plate elements. For instance, using plate elements increases the number of unknowns in the model and complicates the problem-solving, and spring and rod elements cannot approximate the bending behavior of the model while beam elements seem to overcome these issues. The models' beam elements, representing the C-C covalent bonds, have material and geometric properties, which are incorporated in their simulation and the model analysis process. Linking solid mechanics and molecular mechanics has provided an opportunity to calculate such properties successfully, based on an energy approach, by the quantities, called force field constants (k_r, k_θ and k_φ) [68] which are listed in Table 2.

In some research works, the small-scale parameters have been introduced in the modeling based on certain theories, e.g., Cosserat theory [6]. In this research, the classical continuum mechanics has been employed and these effects are not regarded.

In many previous investigations, for creating the space frame-like structure of conventional CNTs, C-C bonds were simulated as 1D beam elements in the FEM packages (Ansys, MSC.Marc or ABAQUS), and a hexagonal unit cell was constructed of six connecting beam elements, according to the geometry of the unit cell. Finally, by copying the unit cell about the principal axis of the CNT, a single ring was created to be copied along the principal axis to model a CNT. Nowadays, the advancement in software development has made materials simulation much easier and faster, compared to the past. In the actual research, the CNTs are modeled by extracting the coordinates of the nodes (carbon atoms) as well as the information about the corresponding connections (elements of the models, representing C-C bonds) from Nanotube Modeler (software specializing in generating the geometry of nanotubes and nanocones) and then, importing such data into the commercial FEM code MSC.Marc (MSC Software Corporation, USA) for further modifications and assigning the materials and geometry properties to create the conventional CNTs and HJCNT models. Finally, the natural frequencies of all models were obtained as an output of dynamic modal analyses.

3. Results and discussion

Vibrational analyses were undertaken on the middle-length HJCNTs with all possible connection types and their corresponding fundamental conventional CNTs with the same constant length of about 15 nm under cantilever boundary conditions. In the first phase of this study, SWCNTs were assumed to be hollow cylinders, and their natural frequencies were analytically calculated and compared with the FEM results to validate the results from this numerical approach. In the second phase, a range for the natural frequency of HJCNTs was acquired from FEM analyses to investigate the influence of several factors affecting their vibrational properties.

3.1. Resonance in conventional CNTs

Analytical and numerical analyses were performed to investigate the vibrational properties of conventional CNTs of all configuration types under the cantilever boundary conditions and their results were compared. For analytical solution, the CNT structures were approximated to be hollow cylinders or tubes of the same lengths, diameters and thicknesses as their corresponding CNTs with the same material properties. Then, the natural frequency of the CNTs was analytically calculated by Eqs. (3) and (4) [36],

$$f = \left(3.5156\Big/2\pi\right)\sqrt{EI/\overline{m}L^4} \quad (3)$$

$$I = \pi\left[(d+t)^4 + (d-t)^4\right]/64 \quad (4)$$

where E, I, $\overline{m}$, and L are the Young's modulus, the second moment of area, the mass per unit length, and the length of the SWCNT, respectively.

Table 2
Material and geometric properties of carbon-carbon covalent bond. (*Source*: Obtained from [70]).

Force Field Constants	E (Young's modulus) $= \frac{{k_r}^2 b}{4\pi k_\theta}$	R_b (bond radius) $= 2\sqrt{\frac{k_\theta}{k_r}}$	$I_{xx} = I_{yy}$ (second moments of area) $= \frac{\pi {R_b}^4}{4}$	A_{C-C} (cross-section area) $= \pi {R_b}^2$
$k_r = 651.97$ nN/nm, $k_\theta = 0.87$ nN·nm/rad^2, $k_\varphi = 0.27$ nN·nm/rad^2	5.48×10^{-6} N/nm^2	0.0733nm	2.2661×10^{-5} nm^4	0.0169 nm^2

Since the investigations are performed in the linear-elastic range, for obtaining Young's modulus, the CNT models were pulled by an arbitrary displacement in the FEM package (MSC.Marc), and the pertaining reaction forces were acquired as an output of the numerical analyses to be used for the calculation of the CNTs' Young's modulus by the following equations [68]:

$$\sigma = \text{stress} = \text{P} \Big/ \text{A} = \frac{\text{reaction force}}{\text{cross} - \text{section area}} \tag{5}$$

$$\varepsilon = \text{strain} = \Delta L \Big/ L = \frac{\text{displacement B.C.}}{\text{length of CNT}} \tag{6}$$

$$E = \text{Young's modulus} = \sigma/\varepsilon \tag{7}$$

In the second phase, the CNTs were simulated as cylinder-shaped space frames in the commercial FEM software, MSC.Marc and their natural frequencies were obtained under cantilever boundary conditions from a modal analysis. Tables 3 to 5 provide the natural frequency of conventional CNTs from analytical and FEM analyses.

The analytical and FEM results in Tables 3 to 5 which are in a good agreement with the literature, e.g., [67], prove the reliability of the employed research method for prediction of the vibrational properties of the CNTs. However, for the relatively very thin CNTs, drift aways are observed between FEM and analytical results. By increasing the chirality or the radius of the 15-nm-long CNTs, an increase in their natural frequencies was observed. On the other hand, the results in the literature demonstrate an exponential decrease in the vibrational stability of the CNTs as result of an increase in their length [43–45]. Such a behavior could also be confirmed by Eq. (4) where such an inverse correlation is seen between the natural frequency of the CNTs and their aspect ratios (L/D) which means that an increase in the length and diameter of the CNTs results in an increase and a decrease in their natural frequencies, respectively.

Based on the FEM results, the natural frequency of SWCNTs lies in the general range of 7.09 and 48.75 GHz. The trends in the results by Hu et al. [32] demonstrated the natural frequency of (5,5) SWCNT of length

Table 3
Natural frequency of conventional armchair carbon nanotubes (n,n).

Chirality	Young's modulus (TPa)	Aspect ratio (L/D)	Natural frequency (GHz)		Relative difference in %
			Analytical	FEM	
(5,5)	1.040	22.13	14.31	12.83	10.32
(6,6)	1.039	18.44	16.63	15.34	7.77
(7,7)	1.040	15.81	19.02	17.84	6.20
(8,8)	1.039	13.83	21.44	20.3	5.19
(9,9)	1.040	12.29	23.90	22.81	4.55
(10,10)	1.038	11.05	26.35	25.28	4.07
(11,11)	1.039	10.06	28.86	27.72	3.94
(12,12)	1.039	9.22	31.36	30.15	3.84
(13,13)	1.040	8.51	33.87	32.56	3.86
(14,14)	1.040	7.90	36.38	34.95	3.93
(15,15)	1.040	7.38	38.90	37.31	4.09
(16,16)	1.039	6.97	40.76	39.03	4.25
(17,17)	1.039	6.56	43.08	41.31	4.11
(18,18)	1.040	6.15	46.49	44.26	4.80
(19,19)	1.040	5.82	49.02	46.52	5.10
(20,20)	1.040	5.53	51.56	48.75	5.45

Table 4
Natural frequency of conventional zigzag carbon nanotubes (n,0).

Chirality	Young's modulus (TPa)	Aspect ratio (L/D)	Natural frequency (GHz)		Relative difference in %
			Analytical	FEM	
(5,0)	0.989	38.27	9.56	7.09	25.83
(6,0)	1.004	31.90	10.77	8.605	20.12
(7,0)	1.014	27.34	12.04	10.10	16.09
(8,0)	1.020	23.92	13.34	11.59	13.14
(9,0)	1.024	21.26	14.68	13.08	10.90
(10,0)	1.027	19.14	16.04	14.55	9.29
(11,0)	1.030	17.40	17.42	16.02	8.03
(12,0)	1.032	15.95	18.81	17.48	7.09
(13,0)	1.033	14.72	20.22	18.94	6.33
(14,0)	1.034	13.67	21.64	20.39	5.76
(15,0)	1.035	12.76	23.06	21.83	5.33
(16,0)	1.036	11.96	24.49	23.27	4.99
(17,0)	1.036	11.26	25.93	24.70	4.73
(18,0)	1.037	10.63	27.37	26.13	4.53
(19,0)	1.037	10.07	28.81	27.55	4.39
(20,0)	1.038	9.57	30.26	28.96	4.30

Table 5
Natural frequency of conventional chiral carbon nanotubes (n,m).

Chirality	Young's modulus (TPa)	Aspect ratio (L/D)	Natural frequency (GHz)		Relative difference in %
			Analytical	FEM	
(7,1)	1.022	25.36	12.70	10.83	14.71
(7,3)	1.038	21.55	14.52	12.93	10.95
(8,3)	1.044	19.44	15.89	14.45	9.06
(9,6)	1.052	14.64	20.44	19.33	5.44
(14,2)	1.050	12.68	23.35	22.20	4.93
(13,4)	1.058	12.44	23.90	22.95	3.97
(11,7)	1.047	12.18	24.07	22.88	4.94
(15,3)	1.051	11.46	25.65	24.61	4.06
(15,4)	1.051	11.04	26.57	25.51	3.97
(14,6)	1.057	10.77	27.29	26.29	3.67
(15,5)	1.047	10.62	27.40	26.21	4.34
(13,8)	1.055	10.43	28.07	27.04	3.67
(9,13)	1.056	10.00	29.23	28.19	3.57
(13,9)	1.052	10.00	29.13	27.99	3.90
(16,7)	1.055	9.38	31.07	29.95	3.60
(19,3)	1.047	9.27	31.25	29.98	4.07
(20,4)	1.053	8.60	33.74	32.54	3.57
(17,10)	1.066	8.11	36.08	35.11	2.68

15 nm up to 50 GHz as well as a decrease in such a quantity as a result of an increase in the model's length. Sakhaee-Pour et al. [34] reported the natural frequencies to vary between 11 and 34 GHz for zigzag and between 23 and 34 for armchair SWCNTs of 13.92–15 nm length under the cantilever boundary conditions. The result was also confirmed by Fakhrabadi et al. [39] who obtained the ranges of $12 < f < 35$ GHz and $13 < f < 35$ GHz for 15 nm long cantilever zigzag and armchair SWCNTs, respectively.

Comparing the results from the current research corresponding to different SWCNT configurations expresses that there is no considerable difference in the natural frequency of the SWCNTs of different configurations with the same aspect ratios. For instance, the natural frequency

of (10,10) armchair model with an aspect ratio of 11.05, (17,0) zigzag model with an aspect ratio of 11.26, and (15,4) chiral model with an aspect ratio of 11.04 was obtained around 25 GHz. This similarity can also be observed for all other models and enlightens the fact that the natural frequency of SWCNTs follows a particular trend in terms of the CNTs' aspect ratio (*AR*) which is expressed by Eq. (8) where *a* and *b* are equal to 254.08 and −0.962 for armchair, 286.53 and −1.012 for zigzag, and 289.86 and −1.013 for chiral models.

$$f = a(AR)^b \tag{8}$$

3.2. Resonance in hetero-junction CNTs

Resonance in HJCNTs with all possible connection types was investigated in the FEM package MSC.Marc under cantilever boundary conditions where one side of the CNTs was fixed and a harmonic load was exerted on the other side to obtain their natural frequencies from modal analyses. With respect to the fact that the HJCNTs were constructed of thinner and wider CNTs, the modal analyses were one time performed when the thinner CNT was fixed and the other time when the wider CNT was fixed to evaluate the influence of the boundary conditions setups on the vibrational properties of the models.

On the other hand, particular SWCNTs, e.g., (10,10) were chosen and considered as the basis of HJCNTs and connected to other SWCNTs of different chiralities and configurations, e.g., (5,5), (7,3) and (15,0) to probe the effect of the connection types on the natural frequency of the resultant HJCNTs, e.g., (10,10)-(5,5), (10,10)-(7,3) and (10,10)-(15,0).

The results in Figs. 2 to 7 demonstrate the natural frequency of middle-length HJCNTs in the general range of 4.04 and 60.20 GHz which are also in a good agreement with the results from literature. For instance, Scarpa et al. [59] studied the vibrational properties of a (5, 5)-(10,10) HJCNT versus length by molecular mechanics, based on which the range of 15 GHz and 260 GHz were acquired as the fundamental frequency of this model with the lengths between 0.5 and 10 nm, respectively. The results from the FEM-based research by Mohammadian et al. [62] demonstrated the natural frequency of HJCNTs between 37 and 46 GHz for clamped-free and, between 126 and 195 GHz for clamped-clamped boundary condition setups. In another investigation, they reported the value of the resonance frequency of clamped-free (3, 3)-(5,5) of 15 nm length and 16.2 nm long (8,8)-(14,14) HJCNTs equal to 14.97 and 35 GHz, respectively. However, for clamped-clamped boundary conditions, 126 GHz was acquired for (8,8)-(14,14). Such results show the influence of the boundary conditions setups on the resonance behavior of HJCNTs. Likewise, FEM-based investigation on straight HJCNTs by Yengejeh et al. [67] proposed the ranges $15 < f < 40$ GHz (when wider CNT is fixed) and $5 < f < 32$ GHz (when thinner CNT is fixed) for armchair-armchair HJCNTs and $12 < f < 17$ GHz (when wider CNT is fixed) and $18 < f < 25$ GHz (when thinner CNT is fixed) for zigzag-zigzag HJCNTs.

Among the research works in the literature, there is little research whose results are different from the results of the current investigation. For example, Yengejeh et al. [67] pointed out that the natural frequency of HJCNTs is within the range of the ones for their fundamental pristine SWCNTs. However, the limitation in the number of HJCNTs and being restricted to only straight models does not seem to be sufficient to reach such a general conclusion.

An overview of such results demonstrates the fact that although the size, orientation and angle of the kinks in the structure of the HJCNTs play role in their vibrational behavior, the boundary condition setups have a determinant influence on the magnitude of the natural frequency of HJCNTs. Comparing results, illustrated in Figs. 2 to 7, clearly shows that higher resonance frequency for cantilever HJCNTs occurs when their wider CNT is clamped when compared to the one when thinner CNT is fixed. Such a conclusion was also made by Motamedi et al. [65].

On the other hand, comparing the natural frequencies of HJCNTs and their fundamental CNTs reveals that for every HJCNT, this quantity for an HJCNT lies outside the natural frequency range of its fundamental CNTs. When the wider CNT is fixed, the natural frequency of HJCNTs appeared to be higher than the ones of their corresponding constituent CNTs and closer to the natural frequency of their corresponding wider tubes. However, when the thinner end of an HJCNT is fixed, such a

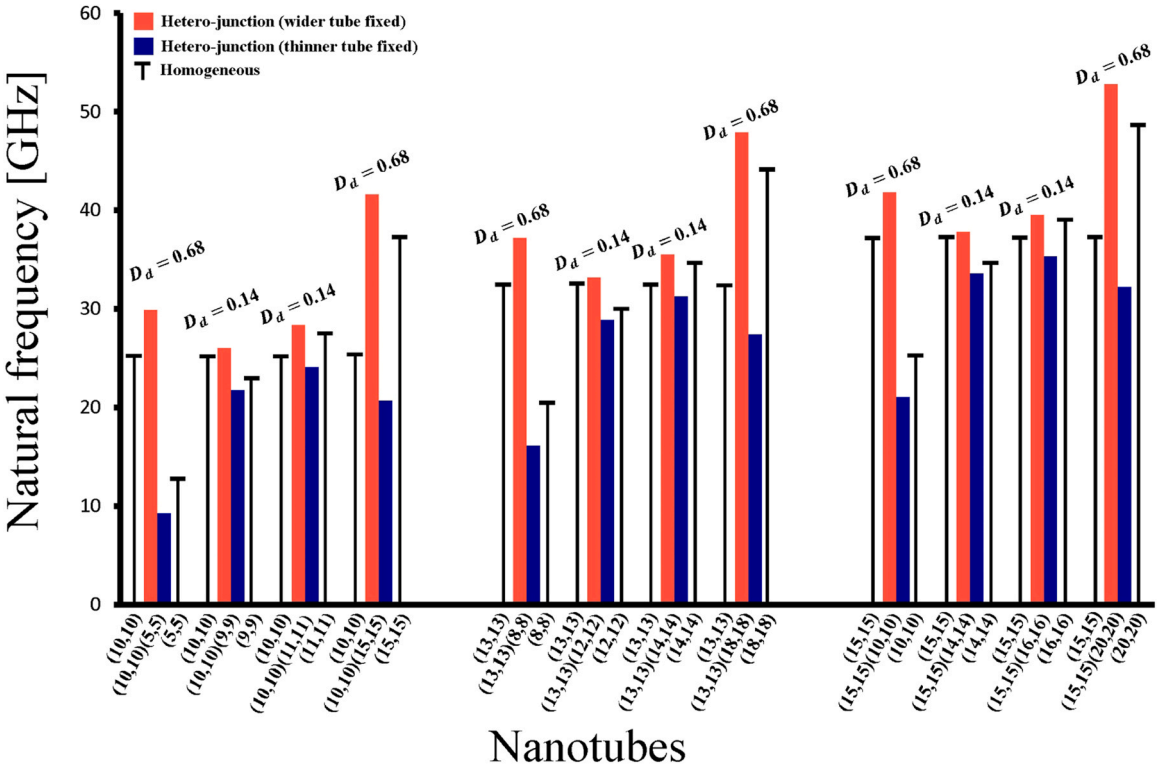

Fig. 2. Natural frequency of armchair-armchair hetero-junction CNTs and their fundamental tubes.

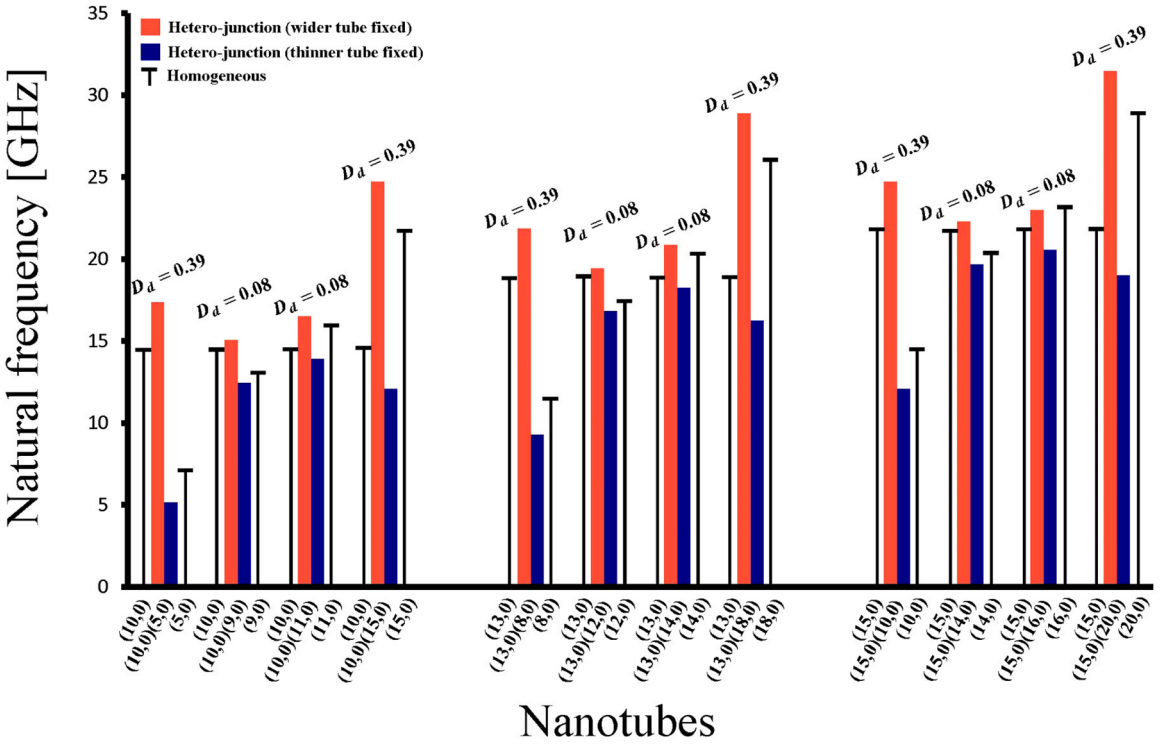

Fig. 3. Natural frequency of zigzag-zigzag hetero-junction CNTs and their fundamental tubes.

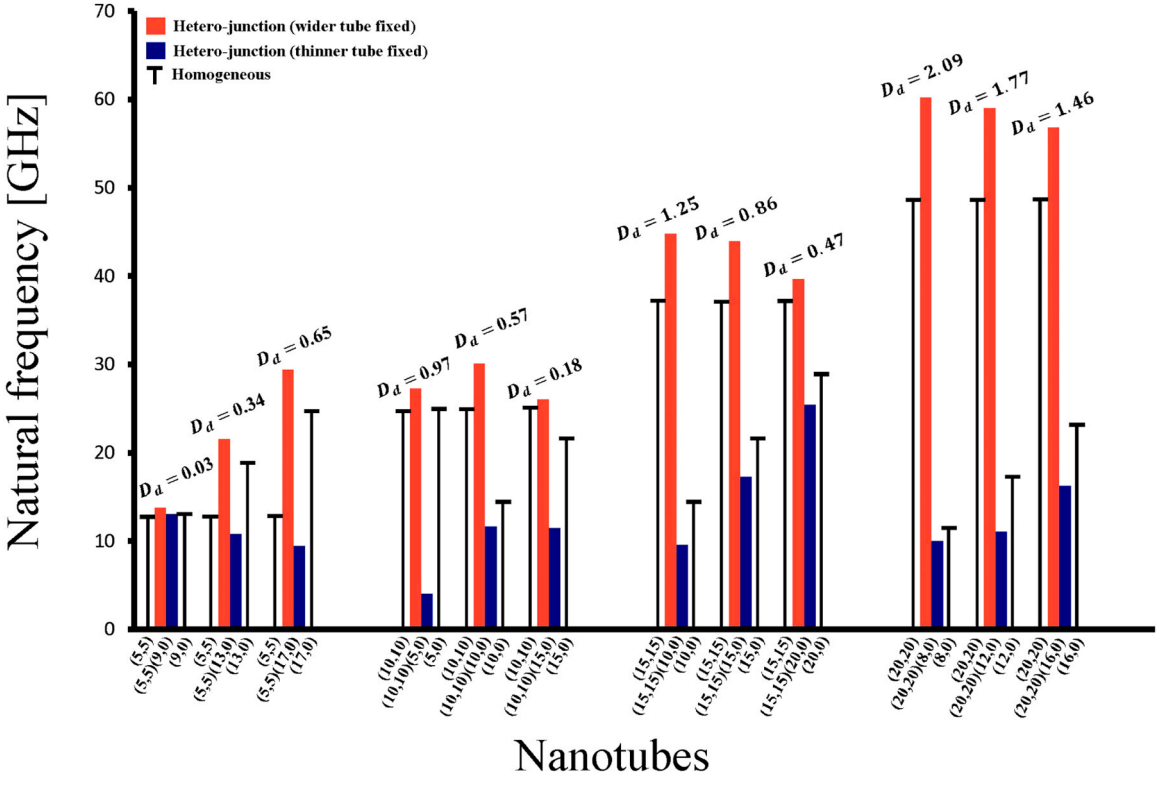

Fig. 4. Natural frequency of armchair-zigzag hetero-junction CNTs and their fundamental tubes.

quantity for almost all the HJCNT models was observed to approach the natural frequency of the pertaining thinner tube and have a smaller value and thus, lower vibrational stability, compared to their corresponding constructive CNTs. This phenomenon could be a result of fixing a higher number of nodes at the wider end of an HJCNT (when the wider tube is fixed) which decreases the mobility of the HJCNT under harmonic load and thus, increases the vibrational stability of the hetero-junction structure. Likewise, fixing the thinner end of an HJCNT will lead to a smaller number of fixed nodes and makes the free vibrating end of the structure more prone to vibrate which causes the whole structure

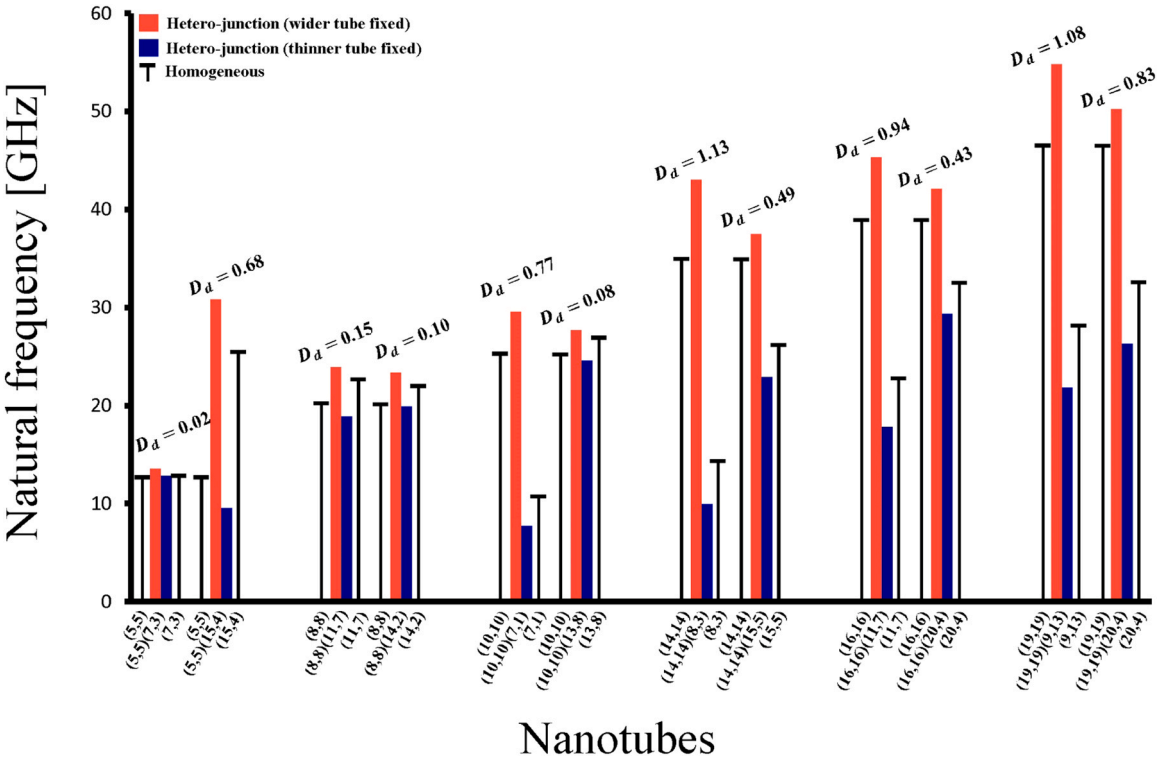

Fig. 5. Natural frequency of armchair-chiral hetero-junction CNTs and their fundamental tubes.

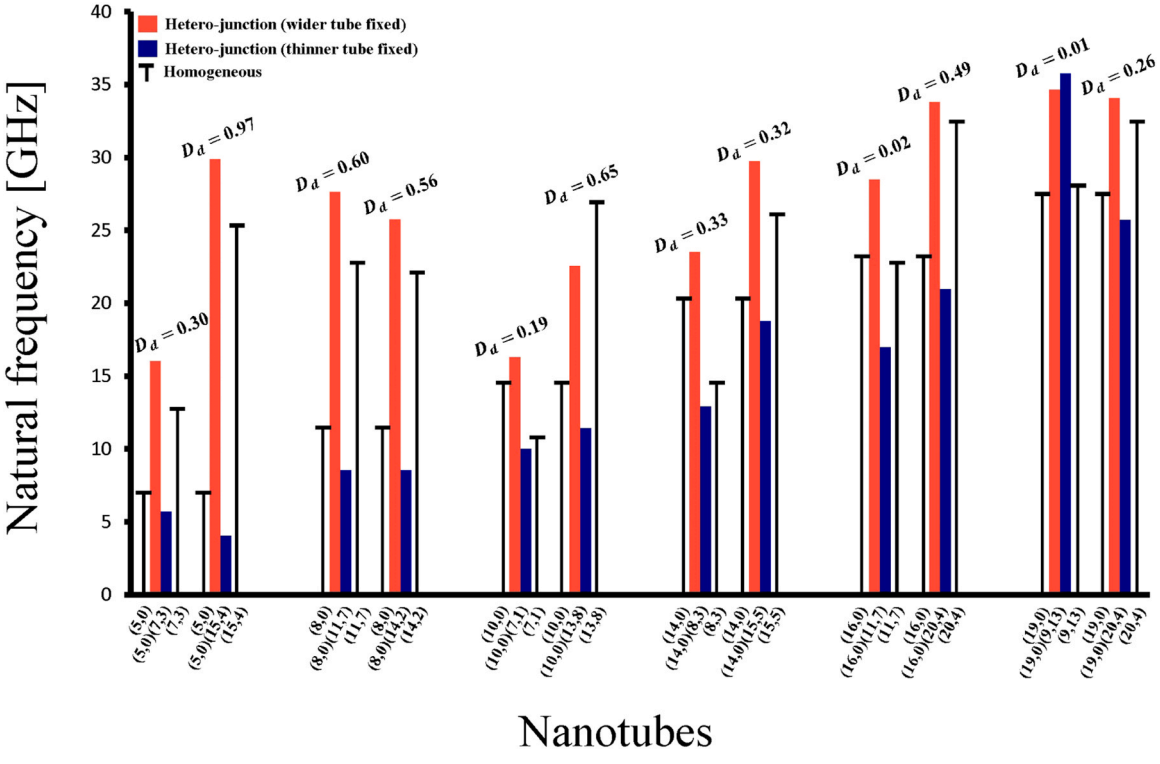

Fig. 6. Natural frequency of zigzag-chiral hetero-junction CNTs and their fundamental tubes.

to experience the resonance sooner and have a relatively lower natural frequency, when compared with its fundamental CNTs. The considerably higher natural frequencies of the HJCNTs under clamped-clamped boundary conditions, reported in the literature, e.g., the research by Mohammadian et al. [62] can similarly be explained as clamped-clamped hetero-structures are more restricted to vibrate, resulting in higher natural frequencies.

The difference between the diameters of the connecting fundamental CNTs (D_d) in the structure of HJCNTs also elucidated a considerable influence on the magnitude of the natural frequency of the resultant

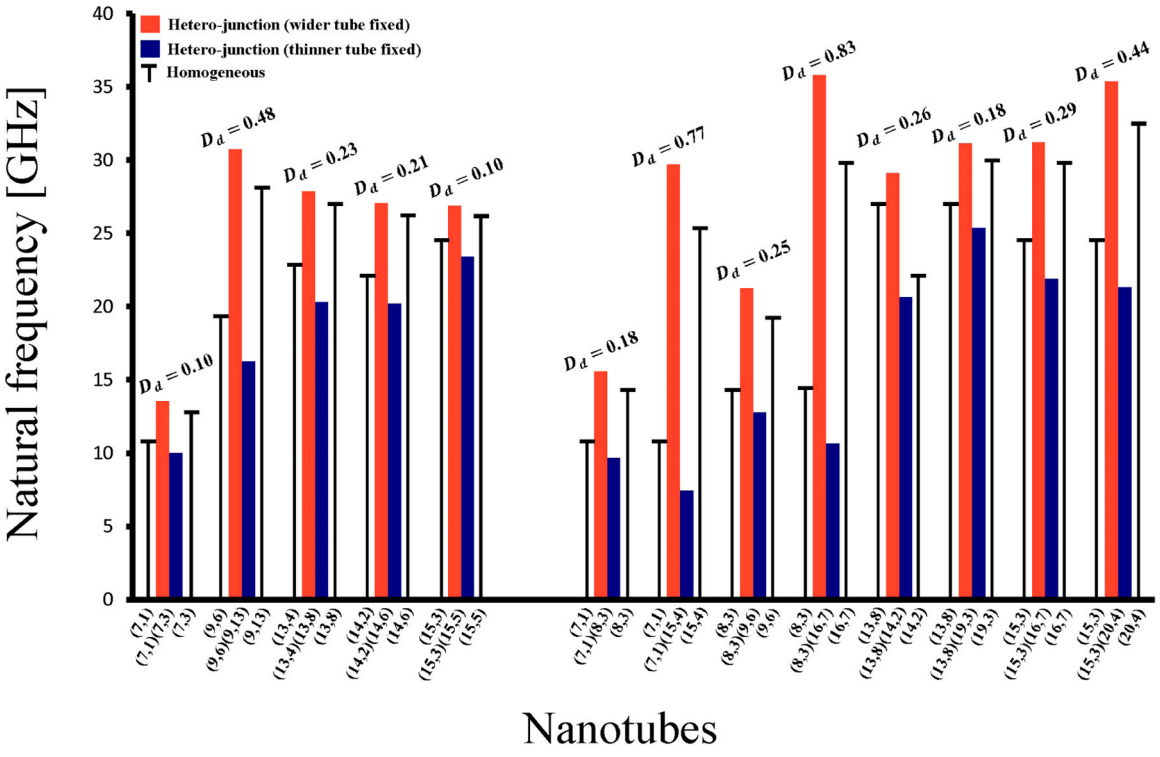

Fig. 7. Natural frequency of chiral-chiral hetero-junction CNTs and their fundamental tubes.

HJCNT. In fact, the larger D_d is, the more the natural frequency of an HJCNT takes distance from the natural frequencies of its fundamental CNTs as a result of decreasing the homogeneity in the HJCNT structure. For instance, as shown in Fig. 2, the difference between the natural frequency of (10,10)-(5,5) with $D_d = 0.68$ nm and the natural frequency of its fundamental CNTs ((10,10) and (5,5)) is greater than such a difference between that of (10,10)-(9,9) with $D_d = 0.14$ nm and the ones for its constructive CNTs ((10,10) and (9,9)).

Among different connection types, the existence of armchair configuration in the structure of HJCNTs with AA, AZ, and AC connections appear to lead to higher natural frequency, ranging from 4.04 to 60.20 GHz when compared with the natural frequency of the models, made of other CNT configurations (ZZ, ZC and CC), ranging between 5.17 and 35.82 GHz. It is generally perceived from the results that the connection between thicker CNTs leads to higher vibrational stability than the connection between thinner CNTs.

4. Conclusion

In summary, the natural frequency of the HJCNTs has not comprehensively been studied in the previous research as the number of the CNT models was insufficient to reach a comprehensive conclusion and only were some hetero-junction types addressed. In the this investigation, FEM approach was utilized to simulate middle-length HJCNTs with all possible connection types, accompanied by their corresponding constructive conventional CNTs to present a more reliable estimated range for the resonance frequency of these nanomaterials and discover the most influential factors affecting their resonance behavior. According to the results, the natural frequency of conventional CNTs varies in the general range of 7.09 and 48.75 GHz and has an inverse correlation to the aspect ratios of the CNTs which follow a particular trend and a mathematical relation was proposed to express such an inverse correlation.

A general range of 4.04 and 60.20 GHz was acquired by the same method for the natural frequency of HJCNTs. The results depict that the natural frequency of an HJCNT generally lies outside the frequency range of its fundamental CNTs and is mainly determined by two factors, i.e., boundary Conditions and the difference between the diameters of the connecting CNTs. Fixing the wider side of the HJCNTs achieves higher natural frequency while fixing their thinner side, leads to lower vibrational stability when compared to the natural frequency of the models' constructive CNTs. On the other hand, the larger the difference between the diameters of the connecting CNTs is, the more the natural frequency of the resultant HJCNT takes distance from the natural frequencies of its fundamental CNTs.

It was also perceived that the existence of armchair CNT in the structure of HJCNTs results in higher resonance frequencies. Eventually, it can be concluded that the natural frequency of HJCNTs is not considerably influenced by the chirality of their constructive CNTs.

With regards to the fact that the actual investigation is limited to the resonance analysis of middle-length HJCNTs under cantilever boundary conditions, the necessity of similar research on the vibrational behavior of short and long HJCNTs is highlighted. Moreover, disregarding the evaluation of the influence of other boundary conditions, e.g., clamped-clamped conditions and the small-scale effects are another gaps to be covered in the future research to establish a comprehensive database for the resonance frequency of HJCNTs for proper selection of these nanomaterials for their potential applications in NEMS, e.g., nanosensors.

CRediT authorship contribution statement

Sourish Banerjee: Writing – review & editing. **Moones Rahmandoust:** Writing – review & editing, Methodology. **Andreas Öchsner:** Writing – review & editing. **Ali Ghavamian:** Writing – original draft, Software, Project administration, Methodology, Investigation, Formal analysis, Data curation, Conceptualization.

Declaration of Competing Interest

The authors would like to confirm that this manuscript has not been submitted to any other journal and contains only new research findings and would declare that they have no known competing financial

interests or personal relationships that could have appeared to influence the work reported in this paper.

Data Availability

No data was used for the research described in the article.

References

[1] S. Iijima, Helical microtubules of graphitic carbon, Nature 354 (1991) 56–58, https://doi.org/10.1038/354056a0.

[2] S. Imani Yengejeh, M. Akbar Zadeh, A. Öchsner, On the buckling behavior of connected carbon nanotubes with parallel longitudinal axes, Appl. Phys. A. 115 (2014) 1335–1344, https://doi.org/10.1007/s00339-013-7999-2.

[3] P. Pancharal, Z.L. Wang, D. Ugarte, W. de Heer, Electrostatic deflections and electromechanical resonances of carbon nanotubes, Science 183 (1999) 1513–1516, https://doi.org/10.1126/science.283.5407.1513.

[4] J. Kong, N.R. Franklin, C.W. Zhou, M.G. Chapline, S. Peng, K.J. Cho, H. Dia, Nanotube molecular wires as chemical sensors, Science 287 (2000) 622–625, https://doi.org/10.1126/science.287.5453.622.

[5] Q.H. Wang, M. Yan, R.P.H. Chang, A nanotube-based field-emission flat panel display, Appl. Phys. Lett. 72 (1998) 2912–2913, https://doi.org/10.1063/1.121493.

[6] P. Kim, C.M. Lieber, Nanotube nanotweezers, Science 285 (1999) 2148–2150, https://doi.org/10.1126/science.286.5447.2148.

[7] H. Dai, J.H. Hafner, A.G. Rinzler, D.T. Ccbert, R.E. Smalley, Nanotubes as nanoprobes in scanning probe microscopy, Nature 384 (1996) 147–150, https://doi.org/10.1038/384147a0.

[8] A.C. Dillon, K.M. Jones, T.A. Bekkedahl, C.H. Kiang, D.S. Bethune, M.J. Heben, Storage of hydrogen in single-walled carbon nanotubes, Nature 386 (1997) 377–379, https://doi.org/10.1038/386377a0.

[9] B.A. Bianco, K. Kostarelos, M. Prato, Applications of carbon nanotubes in drug delivery, Curr. Opin. Chem. Biol. 9 (2005) 674–679, https://doi.org/10.1016/j.cbpa.2005.10.005.

[10] H. Kantamneni, A. Gollakota, Carbon nanotubes based systems for targeted drug delivery: a review (https://doi.org/), Int. J. Eng. Res. Technol. 2 (2013) 1–8, https://doi.org/10.17577/IJERTV2IS2251.

[11] T. Rueckes, K. Kim, E. Joselevich, G.Y. Tseng, C.L. Cheung, C.M. Lieber, Carbon nanotube-base non-volatile random access memory for molecular computing, Science 289 (2000) 94–97, https://doi.org/10.1126/science.289.5476.94.

[12] H.D. Espinosa, C. Ke, N. Pugno, Nanoelectromechanical Systems: Experiments and Modeling, in: K.H.J. Buschow, M.C. Flemings, E.J. Kramer, P. Veyssière, R.W. Cahn, B. Ilschner, S. Mahajan (Eds), Encyclopedia of Materials: Science and Technology (second edition), 2006, pp. 1-9. ⟨https://doi.org/10.1016/B0-08-043152-6/02134-3⟩.

[13] Y. Sun, M. Sun, D. Xie, Graphene Electronic Devices, in: H. Zhu, Z. Xu, D. Xie, Y. Fang (Eds), Graphene Fabrication, Characterizations, Properties and Applications, 2018, pp. 103-155. ⟨https://doi.org/10.1016/B978-0-12-812651-6.00005-7⟩.

[14] M.S.H. Al-Furjan, R. Kolahchi, L. Shan, M.H. Hajmohammad, A. Farrokhian, X. Shen, Slamming impact induced hydrodynamic response in wave-piercing catamaran beam elements with controller, Ocean. Eng. 266 (2022) e112908, https://doi.org/10.1016/j.oceaneng.2022.112908.

[15] M. Mohammadimehr, S. Alimirzae, Nonlinear static and vibration analysis of Euler-Bernoulli composite beam model reinforced by FG-SWCNT with initial geometrical imperfection using FEM, Struct. Eng. Mech. 59 (2016) 431–454, https://doi.org/10.12989/sem.2016.59.3.431.

[16] H. Mellouli, H. Jrad, M. Wali, F. Dammak, Free vibration analysis of FG-CNTRC shell structures using the meshfree radial point interpolation method, Comput. Math. Appl. 79 (2020) 3160–3178, https://doi.org/10.1016/j.camwa.2020.01.015.

[17] N.D. Dat, T.Q. Quan, V. Mahesh, N.D. Duc, Analytical solutions for nonlinear magneto-electro-elastic vibration of smart sandwich plate with carbon nanotube reinforced nanocomposite core in hygrothermal environment, Int. J. Mech. Sci. 186 (2020) e105906, https://doi.org/10.1016/j.ijmecsci.2020.105906.

[18] A. Ghorbanpour Arani, M. Mosayyebi, F. Kolahdouzan, R. Kolahchi, M. Jamali, Refined zigzag theory for vibration analysis of viscoelastic functionally graded carbon nanotube reinforced composite microplates integrated with piezoelectric layers, Proc. Inst. Mech. Eng., Part G: J. Aerosp. Eng. 231 (2016) 2464–2478, https://doi.org/10.1177/0954410016667150.

[19] L. Shan, C.Y. Tan, X. Shen, S. Ramesh, M.S. Zarei, R. Kolahchi, M. H. Hajmohammad, The effects of nano-additives on the mechanical, impact, vibration, and buckling/post-buckling properties of composites: A review, J. Mater. Res. Technol. 24 (2023) 7570–7598, https://doi.org/10.1016/j.jmrt.2023.04.267.

[20] P.H. Wan, M.S.H. Al-Furjan, R. Kolahchi, L. Shan, Application of DQHFEM for free and forced vibration, energy absorption, and post-buckling analysis of a hybrid nanocomposite viscoelastic rhombic plate assuming CNTs' waviness and agglomeration, Mech. Syst. Signal. Process. 189 (2023) e110064, https://doi.org/10.1016/j.ymssp.2022.110064.

[21] H. Wang, C.S. Chen, C.Y. Hsu, W.R. Chen, Vibration and stability of initially stressed functionally graded carbon nanotube-reinforced hybrid composite plates in thermal environments, Mech. Base. Des. Struct. Mach. 50 (2020) 1298–1313, https://doi.org/10.1080/15397734.2020.1749070.

[22] J. Fazilati, V. Khalafi, M. Jalalvand, Free vibration analysis of three-phase CNT/polymer/fiber laminated tow-steered quadrilateral plates considering agglomeration effects, Thin-Walled. Struct. 179 (2022) e109638, https://doi.org/10.1016/j.tws.2022.109638.

[23] H. Babaei, Free vibration and snap-through instability of FGCNTRC shallow arches supported on nonlinear elastic foundation, Appl. Math. Comput. 413 (2022) e126606, https://doi.org/10.1016/j.amc.2021.126606.

[24] R. Nopour, F. Ebrahimi, A. Dabbagh, M.M. Aghdam, Nonlinear forced vibrations of three-phase nanocomposite shells considering matrix rheological behavior and nano-fiber waviness, Eng. Comput. 39 (2023) 557–574, https://doi.org/10.1007/s00366-022-01608-7.

[25] A. Ghavamian, A. Öchsner, On the buckling behavior of perfect and atomically defective hetero-junction carbon nanotubes, Mech. Adv. Mater. Struct. 24 (2017) 1043–1057, https://doi.org/10.1080/15376494.2016.1202360.

[26] A. San Paulo, J. Black, D. Garcıía-Sanchez, M.J. Esplandiu, A. Aguasca, J. Bokor, F. Perez-Murano, A. Bachtold, Mechanical detection and mode shape imaging of vibrational modes of micro and nanomechanical resonators by dynamic force microscopy, J. Phys. Conf. Ser. 100 (2008) 1–5, https://doi.org/10.1088/1742-6596/100/5/052009.

[27] R. Ansari, S. Sahmani, Small scale effect on vibrational response of single-walled carbon nanotubes with different boundary conditions based on nonlocal beam models, Commun. Nonlinear Sci. Numer. Simula 17 (2012) 1965–1979, https://doi.org/10.1016/j.cnsns.2011.08.043.

[28] U. Lee, H. Oh, S. You, Natural Frequencies of Single-Walled Carbon Nanotubes, Proceedings of the 2nd IEEE International, Conference on Nano/Micro Engineered and Molecular Systems, Bangkok, Thailand, (2007) 13-16. ⟨https://doi.org/10.1109/NEMS.2007.352240⟩.

[29] J.N. Lu, H.B. Chen, P. Lu, P.Q. Zhang, Research of natural frequency of single-walled carbon nanotube, Chin. J. Chem. Phys. 20 (2007) 525–530, https://doi.org/10.1088/1674-0068/20/05/525-530.

[30] C. Li, T.W. Chou, Single-walled carbon nanotubes as ultrahigh frequency nanomechanical resonators, Phys. Rev. B. 68 (2003) e073405, https://doi.org/10.1103/PhysRevB.68.073405.

[31] R. Chowdhury, S. Adhikari, C.Y. Wanga, F. Scarpa, A molecular mechanics approach for the vibration of single-walled carbon nanotubes, Comput. Mater. Sci. 48 (2010) 730–735, https://doi.org/10.1016/j.commatsci.2010.03.020.

[32] Y.G. Hu, K.M. Liew, Q. Wang, Modeling of vibrations of carbon nanotubes, Procedia Eng. 31 (2012) 343–347, https://doi.org/10.1016/j.proeng.2012.01.1034.

[33] C.W. Fan, Y.Y. Liu, C. Hwu, Finite element simulation for estimating the mechanical properties of multi-walled carbon nanotubes, Appl. Phys. A. 95 (2009) 819–831, https://doi.org/10.1007/s00339-009-5080-y.

[34] A. Sakhaee-Pour, M.T. Ahmadian, A. Vafai, Vibrational analysis of single-walled carbon nanotubes using beam element, Thin-Wall. Struct. 47 (2009) 646–652, https://doi.org/10.1016/j.tws.2008.11.002.

[35] M. Mir, A. Hosseini, G.H. Majzoobi, A numerical study of vibrational properties of single-walled carbon nanotubes, Comput. Mater. Sci. 43 (2008) 540–548, https://doi.org/10.1016/j.commatsci.2007.12.024.

[36] M. Rahmandoust, A. Öchsner, Buckling behavior and natural frequency of zigzag and armchair single-walled carbon nanotubes, J. Nano. Res. 16 (2011) 153–160, https://doi.org/10.4028/www.scientific.net/JNanoR.16.153.

[37] A. Ghavamian, A. Öchsner, Numerical modeling of eigenmodes and eigenfrequencies of single-and multi-walled carbon nanotubes under the influence of atomic defects, Comput. Mater. Sci. 72 (2013) 42–48, https://doi.org/10.1016/j.commatsci.2013.02.002.

[38] S. Arghavan, A.V. Singh, On the vibrations of single-walled carbon nanotubes, Thin-Wall. Struct. 47 (2009) 646–652, https://doi.org/10.1016/j.jsv.2011.01.032.

[39] M.M.S. Fakhrabadi, M. Samadzadeh, A. Rastgoo, M.H. Yazdi, M.M. Mashhadi, Vibrational analysis of carbon nanotubes using molecular mechanics and artificial neural network, Low. -Dimens. Syst. Nanostruct. 44 (2011) 565–578, https://doi.org/10.1016/j.physe.2011.10.004.

[40] Z. Ebrahim Zadeh, M. Yadollahpour, S. Ziaei-Rad, F. Karimzadeh, The effect of vacancy defects and temperature on fundamental frequency of single walled carbon nanotubes, Comput. Mater. Sci. 63 (2012) 12–19, https://doi.org/10.1016/j.commatsci.2012.05.045.

[41] M.M. Selim, S.A. El-Safty, Vibrational analysis of an irregular single-walled carbon nanotube incorporating initial stress effects, Nanotechnol. Rev. 9 (2020) 1481–1490, https://doi.org/10.1515/ntrev-2020-0114.

[42] V. Parvaneh, M. Shariati, H. Torabi, Frequency analysis of perfect and defective SWCNTs, Comput. Mater. Sci. 50 (2011) 2051–2056, https://doi.org/10.1016/j.commatsci.2011.02.007.

[43] M. Chwal, Nonlocal Analysis of Natural Vibrations of Carbon Nanotubes, J. Mater. Eng. Perform. 27 (2018) 6087–6096, https://doi.org/10.1007/s11665-018-3673-3.

[44] D. Miyashiro, H. Taira, R. Hamano, R.L. Reserva, K. Umemura, Mechanical vibration of single-walled carbon nanotubes at different lengths and carbon nanobelts by modal analysis method, Compos. C. 2 (2020) e100028, https://doi.org/10.1016/j.jcomc.2020.100028.

[45] A. Fatahi-Vajari, Z. Azimzadeh, Natural Frequency of Rotating Single-Walled Carbon Nanotubes with Considering Gyroscopic, Eff., J. Solid. Mech. 12 (2020) 136–147, https://doi.org/10.22034/jsm.2019.1866624.1424.

[46] Y. Yao, Q. Li, J. Zhang, R. Liu, L. Jiao, Y.T. Zhu, Z. Liu, Temperature-mediated growth of single-walled carbon-nanotube intramolecular junctions, Nat. Mater. 6 (2007) 283–286, https://doi.org/10.1038/nmat1865.

[47] G.W. Ho, A.T.S. Wee, J. Lin, Electric field-induced carbon nanotube junction formation, Appl. Phys. Lett. 79 (2001) 260–262, https://doi.org/10.1063/1.1383279.
[48] C. Jin, K. Suenaga, S. Iijima, Plumbing carbon nanotubes, Nat. Nano. 3 (2008) 17–21, https://doi.org/10.1038/nnano.2007.406.
[49] L. Chico, V.H. Crespi, L.X. Benedict, S.G. Louie, M.L. Cohen, Pure carbon nanoscale devices: nanotube heterojunctions, Phys. Rev. Lett. 76 (1996) 971–974, https://doi.org/10.1103/PhysRevLett.76.971.
[50] G. Arora, S.I. Sandler, Nanoporous carbon membranes for separation of nitrogen and oxygen: Insight from molecular simulations, Fluid Ph. Equilib. 259 (2007) 3–8, https://doi.org/10.1016/j.fluid.2007.04.013.
[51] M.M.S. Fakhrabadi, A. Amini, A. Rastgoo, Vibrational properties of two and three junctioned carbon nanotubes, Comput. Mater. Sci. 65 (2012) 411–425, https://doi.org/10.1016/j.commatsci.2012.08.002.
[52] H. Wang, X. Bai, J. Wei, P. Li, Y. Jia, H. Zhu, K. Wang, D. Wu, Preparation of CuI particles and their applications in carbon nanotube-Si heterojunction solar cells, Mater. Lett. 79 (2012) 106–108, https://doi.org/10.1016/j.matlet.2012.03.114.
[53] Y. Jia, J. Wei, K. Wang, A. Cao, Q. Shu, X. Gui, Y. Zhu, D. Zhuang, G. Zhang, B. Ma, L. Wang, W. Liu, Z. Wang, J. Luo, D. Wu, Nanotube–Silicon Heterojunction Solar Cells, Adv. Mater. 20 (2008) 4594–4598, https://doi.org/10.1002/adma.200801810.
[54] A. Ghavamian, A. Öchsner, Numerical investigation on the influence of defects on the buckling behavior of single-and multi-walled carbon nanotubes, Phys. E Low. -Dimens. Syst. Nanostruct. 46 (2012) 241–249, https://doi.org/10.1016/j.physe.2012.08.002.
[55] K. Duan, L. Li, Y. Hu, X. Wang, Pillared graphene as an ultra-high sensitivity mass sensor, Sci. Rep. 7 (2017) e14012, https://doi.org/10.1038/s41598-017-14182-6.
[56] K. Duan, Y. Li, L. Li, Y. Hu, X. Wang, Diamond nanothread based resonators: ultrahigh sensitivity and low dissipation, Nanoscale 10 (2018) 8058–8065, https://doi.org/10.1039/C8NR00502H.
[57] A.K. Naik, M. Hanay, W. Hiebert, X. Feng, M.L. Roukes, Towards single-molecule nanomechanical mass spectrometry, Nat. Nanotechnol. 4 (2009) 445–450, https://doi.org/10.1038/nnano.2009.152.
[58] F. Scarpa, J. Narojczyk, K.W. Wojciechowski, D.J. Inman, Self-filtering oscillations in carbon nanotube hetero-junctions, Nanotechnol 22 (2011) e465501, https://doi.org/10.1088/0957-4484/22/46/465501.
[59] F. Scarpa, J. Narojczyk, K.W. Wojciechowski, D.J. Inman, Carbon nanotube hetero-junctions: unusual deformations and mechanical vibration properties, Nanosensors. Biosens. Info-Tech. Sens. Sys 7980 (2011) e798006, https://doi.org/10.1117/12.881914.
[60] M. Mohammadian, M.H. Abolbashari, S.M. Hosseini, Application of hetero junction CNTs as mass nanosensor using nonlocal strain gradient theory: An analytical solution, Appl. Math. Model. 76 (2019) 26–49, https://doi.org/10.1016/j.apm.2019.05.056.
[61] S. Filiz, M. Aydogdu, Axial vibration of carbon nanotube heterojunctions using nonlocal elasticity, Comput. Mater. Sci. 49 (2010) 619–627, https://doi.org/10.1016/j.commatsci.2010.06.003.
[62] M. Mohammadian, M.H. Abolbashari, S.M. Hosseini, The effects of connecting region length on the natural frequencies of straight and non-straight hetero-junction carbon nanotubes, Comput. Mater. Sci. 122 (2016) 11–21, https://doi.org/10.1016/j.commatsci.2016.05.005.
[63] M. Mohammadian, S.M. Hosseini, M.H. Abolbashari, Free vibration analysis of dissimilar connected CNTs with atomic imperfections and different locations of connecting region, Phys. B: Condens. Matt. 524 (2017) 34–46, https://doi.org/10.1016/j.physb.2017.08.045.
[64] M. Mohammadian, S.M. Hosseini, M.H. Abolbashari, Lateral vibrations of embedded hetero-junction carbon nanotubes based on the nonlocal strain gradient theory: Analytical and differential quadrature element (DQE) methods, Phys. E: Low. -Dimens. Sys. Nanostruct. 105 (2019) 68–82, https://doi.org/10.1016/j.physe.2018.08.022.
[65] M. Motamedi, M.Mousavi Mashhadi, A. Rastgoo, Vibration Behavior and Mechanical Properties of Carbon Nanotube Junction, J. Comput. Theor. Nanosci. 10 (2013) 1033–1037, https://doi.org/10.1166/jctn.2013.2803.
[66] A. Roy, K.K. Gupta, S. Dey, Probabilistic investigation of temperature dependent vibrational behavior of BNNT and CNT based hetero-structures, Appl. Nanosci. 12 (2022) 2077–2089, https://doi.org/10.1007/s13204-022-02487-6.
[67] S. Imani Yengejeh, M. Akbar Zadeh, A. Öchsner, Numerical modeling of eigenmodes and eigenfrequencies of hetero-junction carbon nanotubes with pentagon–heptagon pair defects, Comput. Mater. Sci. 92 (2014) 76–83, https://doi.org/10.1016/j.commatsci.2014.05.015.
[68] A. Ghavamian, M. Rahmandoust, A. Öchsner, A numerical evaluation of the influence of defects on the elastic modulus of single and multi-walled carbon nanotubes, Comput. Mater. Sci. 62 (2012) 110–116, https://doi.org/10.1016/j.commatsci.2012.05.003.
[69] A. Ghavamian, M. Rybachuk, A. Öchsner, Defects in carbon nanotubes, in: J. Stehr, I. Buyanova, W. Chen (Eds.), Defects in advanced electronic materials and novel low dimensional structures, Woodhead Publishing, Duxford, 2018, pp. 87–136.
[70] A. Ghavamian, M. Rahmandoust, A. Öchsner, On the determination of the shear modulus of carbon nanotubes, Compos. B Eng. 44 (2013) 52–59, https://doi.org/10.1016/j.compositesb.2012.07.040.
[71] R. Saito, G. Dresselhaus, M.S. Dresselhaus, Tunneling conductance of connected carbon nanotubes, Phys. Rev. B 53 (1996) 2044–2050, https://doi.org/10.1103/PhysRevB.53.2044.
[72] A. Ghavamian, A. Andriyana, A.B. Chin, A. Öchsner, Numerical investigation on the influence of atomic defects on the tensile and torsional behavior of hetero-junction carbon nanotubes, Mater. Chem. Phys. 164 (2015) 122–137, https://doi.org/10.1016/j.matchemphys.2015.08.033.
[73] A. Ghavamian, A. Öchsner, A comprehensive numerical investigation on the mechanical properties of hetero-junction carbon nanotubes, Commun. Theor. Phys. 64 (2015) 215–230. ⟨https://ctp.itp.ac.cn/EN/Y2015/V64/I02/215⟩.
[74] Ph Lambin, A. Fonseca, J.P. Vigneron, J.B. Nagy, A.A. Lucas, Structural and electronic properties of bent carbon nanotubes, Chem. Phys. Lett. 245 (1995) 85–89, https://doi.org/10.1016/0009-2614(95)00961-3.
[75] A. Ghavamian, M. Rahmandoust, A. Öchsner, Numerical Nanomechanics of Perfect and Defective Hetero-junction CNTs, in: R. Pethig, H.D. Espinosa (Eds.), Advanced Computational Nanomechanics, John Wiley & Sons, West Sussex, 2016, pp. 147–174.